Origin and Evolution of Prebiotic Organic Matter As Inferred from the Tagish Lake Meteorite

Christopher D. K. Herd,[1]* Alexandra Blinova,[1] Danielle N. Simkus,[1] Yongsong Huang,[2] Rafael Tarozo,[2] Conel M. O'D. Alexander,[3] Frank Gyngard,[3] Larry R. Nittler,[3] George D. Cody,[4] Marilyn L. Fogel,[4] Yoko Kebukawa,[4] A. L. David Kilcoyne,[5] Robert W. Hilts,[6] Greg F. Slater,[7] Daniel P. Glavin,[8] Jason P. Dworkin,[8] Michael P. Callahan,[8] Jamie E. Elsila,[8] Bradley T. De Gregorio,[9,10] Rhonda M. Stroud[10]

The complex suite of organic materials in carbonaceous chondrite meteorites probably originally formed in the interstellar medium and/or the solar protoplanetary disk, but was subsequently modified in the meteorites' asteroidal parent bodies. The mechanisms of formation and modification are still very poorly understood. We carried out a systematic study of variations in the mineralogy, petrology, and soluble and insoluble organic matter in distinct fragments of the Tagish Lake meteorite. The variations correlate with indicators of parent body aqueous alteration. At least some molecules of prebiotic importance formed during the alteration.

Carbonaceous chondrite meteorites are samples of kilometer-sized primitive asteroids that preserve to varying degrees the initial solid components of the solar protoplanetary disk [or nebula (*1*)]. As such, these meteorites are samples of the material that took part in planet formation nearly 4.6 billion years ago. The chondrites also preserve a record of the processes that occurred in their asteroid parent bodies, such as thermal metamorphism, aqueous alteration, and impact brecciation (*1*). Organic matter composes up to several weight percent of carbonaceous chondrites and includes macromolecular material and a variety of simpler molecules (*2*) that are generally referred to as insoluble organic matter (IOM) and soluble organic matter (SOM), respectively, because of their relative solubilities in typical solvents (*3, 4*). Organic matter in carbonaceous chondrites shares characteristics with material from other primitive extraterrestrial samples, including interplanetary dust particles (IDPs), samples of comet 81P/Wild 2 (*5*, *6*), and some Antarctic micrometeorites (*7*). The common features of IOM from carbonaceous chondrites and comets suggest that there was a common source of such organic matter—the outer solar nebula and/or the interstellar medium—and that the diversity of organic matter in meteorites is the result of variable degrees of parent body modification (*8*).

Earth's carbon was provided by the accretion of early solar system solids. The accretion of meteorites and other asteroidal and cometary material by the early Earth may have been a source of intact organic matter that was necessary for the advent of life (*9*). Carbonaceous chondrite SOM includes molecules of prebiotic interest such as amino acids, nucleobases, monocarboxylic acids (MCAs), sugars, and polycyclic aromatic hydrocarbons (*3*). Some of these compounds may be the result of hydrothermal alteration of IOM in the meteorite parent bodies (*10*–*12*), but which compounds formed in this manner is an open question.

Here we report on IOM and SOM in several individual stones of the Tagish Lake meteorite shower (*13*) that have experienced different levels of hydrothermal alteration (*14*). The meteorite is an ungrouped type 2 carbonaceous chondrite (it has affinities to both CI and CM meteorites) consisting of chondrules set in a fine-grained matrix that is dominated by serpentine and saponite clay minerals (*15*), and it has been linked to the primitive D-type asteroids (*16*). Lithological variability on the scale of individual stones may be attributable to different conditions of alteration and/or impact brecciation (*15*). The Tagish Lake meteorite contains a high concentration of organic matter, nearly 3 weight percent (wt %) (*17*). An unusual distribution of soluble organic compounds that are dominated by carboxylic and sulfonic acids, with only trace (part-per-billion) levels of amino acids, has previously been reported for the Tagish Lake meteorite, suggesting a distinct pathway of organic synthesis as compared to CI and CM meteorites (*18*, *19*). Sub–micrometer-scale carbonaceous globules that are often substantially enriched in ^{15}N and D and are thought to have formed in the interstellar medium or the cold outer solar nebula were previously identified in the Tagish Lake meteorite (*5*, *20*), demonstrating the preservation of such material in spite of parent body alteration.

Terrestrial contamination and modification, both abiotic and biotic, are perennial concerns in the study of meteorite organics. The first Tagish Lake meteorite specimens fell on a frozen lake, were collected without hand contact within a few days of the fall, and have been kept frozen ever since (*21*), providing an opportunity for the study of organic matter in a pristine meteorite sample. Much of what is known about the Tagish Lake meteorite derives from studies of this pristine material (*18, 22*). However, only a handful of the 48 pristine stones have been examined in detail (*21*). We selected four specimens from among these stones on the basis of their macroscopic properties, in order to carry out a systematic study of the variations in organic matter in this meteorite and to test whether variations in IOM or SOM correlate with petrologic differences. We processed subsamples of each of the four specimens (5b, mass 4.3 g; 11h, 6.2 g; 11i, 4.7 g; and 11v, 5.6 g) in parallel, providing extracts for the analysis of SOM and IOM separates, material for x-ray diffraction, and polished mounts for microbeam analyses (*13*).

All four specimens are composed of olivine- and pyroxene-bearing chondrules and chondrule-like objects, compact lithic fragments, and isolated olivine or pyroxene grains, set in a fine-grained porous matrix dominated by clays, sulphides, magnetite, and carbonates. Based on the relative proportions of porous matrix and framboidal magnetite (*15*), and the increasing replacement of chondrule glass by phyllosilicates (*23*), the degree to which the specimens have undergone aqueous alteration is in the order 5b < 11h << 11i. Specimen 11v, which consists of disaggregated material collected from the lake ice surface, is heterogeneous on the microscale, comprising clasts whose petrologic

[1]Department of Earth and Atmospheric Sciences, University of Alberta, Edmonton, Alberta T6G 2E3, Canada. [2]Department of Geological Sciences, Brown University, 324 Brook Street, Providence, RI 02912, USA. [3]Department of Terrestrial Magnetism, 5241 Broad Branch Road, Carnegie Institution of Washington (CIW), Washington, DC 20015, USA. [4]Geophysical Laboratory, 5251 Broad Branch Road, CIW, Washington, DC 20015, USA. [5]Advanced Light Source, Lawrence Berkeley Laboratory, Berkeley, CA 94720, USA. [6]Department of Physical Sciences, Grant MacEwan University, Edmonton, Alberta T5J 4S2, Canada. [7]School of Geography and Earth Sciences, McMaster University, Hamilton, Ontario L8S 4K1, Canada. [8]NASA Goddard Space Flight Center, Greenbelt, MD 20771, USA. [9]Engineering and Science Contract Group, NASA Johnson Space Center, Houston, TX 77058, USA. [10]Naval Research Laboratory, 4555 Overlook Avenue SW, Washington, DC 20375, USA.

*To whom correspondence should be addressed. E-mail: herd@ualberta.ca

Table 1. Summary of results of IOM analysis of Tagish Lake specimens. See (*41*). Previous data are from (*8*).

Sample	Previous	11v	11i	11h	5b
C (wt %)	~2	1.77(9)	1.82(4)	1.86	1.6(3)
H/C (at.)	0.337	0.44(1)	0.51(2)	0.594	0.72(4)
N/C (at.)	0.043(2)	0.041(1)	0.042(2)	0.042	0.042(2)
$\delta^{13}C$ (‰)	−14.2(1)	−13.3	−13.3(1)	−14.3	−14.7(2)
$\delta^{15}N$ (‰)	73(2)	58(2)	53(1)	57	57(4)
δD (‰)	596(4)	815(25)	992(15)	1470	1844(10)

characteristics cover the range seen in the other three specimens. The macroscopic differences among the specimens are attributable to the proportions of the various components, as well as matrix grain size. For example, 11i, which is very dark and tends to shed a residue of black dust, has a lower proportion of chondrules and a smaller average matrix grain size (<5 μm).

Isotopic and chemical analyses of bulk IOM separates from each of the four specimens (Table 1 and Fig. 1A) show that the largest variations are in the H/C ratios and H isotopic compositions (δD); variations in N isotopic compositions and in C in IOM as a proportion of the rock are negligible. C isotopic compositions show a small but substantial increase in the order 5b > 11h > 11i ~ 11v (Table 1). The variations in H/C and δD observed in IOM in these specimens span almost the entire range found among the different carbonaceous chondrite groups (Fig. 1A). This lends credence to the suggestion that the variation in IOM elemental and isotopic compositions found in chondrites is the result of parent body modification of a common precursor (*8*). Furthermore, there is a linear correlation between H/C ratios and δD values (Fig. 1). Solid-state ^{13}C and ^{1}H nuclear magnetic resonance spectroscopy and carbon x-ray absorption near-edge spectroscopy [C-XANES (*24*)] (*13*) indicate that the decrease in the H/C ratio is accompanied by an increase in the proportion of aromatic C in the IOM as well as a considerable increase in aromatic substitution, probably aromatic condensation (*13*). The change in H/C was not accompanied by a substantial loss of C (Table 1), which may indicate that the aliphatic component in the Tagish Lake meteorite was converted into aromatic C, while undergoing H isotopic exchange with the altering fluid and/or preferential D loss. This apparently facile transformation is unexpected. It is most likely caused by hydrothermal alteration, as is observed in experiments involving hydrous pyrolysis or reaction with water at elevated temperature and pressure (*11*, *25*), and differs from the scenario in which aliphatic C is selectively removed through reaction with an oxidant (*26*).

High-spatial-resolution secondary ion mass spectroscopic (SIMS) measurements reveal that the isotopic differences observed in bulk IOM residues extend to submicrometer scales. IOM from sample 5b shows not only a higher average D/H ratio but also a much higher proportion of very D-rich submicrometer-sized isotopic hot spots (Fig. 1B) with more extreme D/H ratios than those from 11v [maximum δD ~20,000 per mil (‰) in 5b versus ~7000‰ in 11v]. These observations suggest that parent body alteration has substantially removed D, decreasing the D/H ratio on all spatial scales and reducing the number of hot spots. Similar variations in D enrichments and abundances between chondrites have been observed before, but never in a single chondrite. In contrast, the N isotopic distributions are similar except that 5b contains about twice the number density of ^{15}N hot spots (with $\delta^{15}N$ in both residues up to ~800‰). This difference in behavior of H and N isotopes supports observations in previous studies that D and ^{15}N enrichments in IOM tend to be decoupled (*5*). Isotopic hot spots are, in many cases, associated with carbonaceous nanoglobules (*5*, *20*). Transmission electron microscope (TEM) examinations indicate that IOM from sample 5b has a significantly higher fraction (7.5%) of nanoglobules than does IOM from 11v (0.9%) (*13*). C-XANES (*24*) indicates the presence of two chemical classes of nanoglobules, one with a C functional group distribution similar to that in nonglobular IOM and one dominated by aromatic functionality (*13*). Aromatic-type nanoglobule spectra are seen in a higher fraction of nanoglobules from 11v as compared to 5b [50% versus 20% (*13*)]. Taken together, the SIMS, TEM, and XANES results suggest that ^{15}N-rich nanoglobules have been preferentially destroyed in specimen 11v by hydrothermal alteration. Moreover, the higher fraction of highly aromatic nanoglobules in the more altered sample supports the conclusion from the bulk data that the alteration largely affects the aliphatic component of the IOM.

Based on IOM results, the degree of alteration reflected by the Tagish Lake specimens is 5b < 11h < 11i < 11v, which is consistent with the order inferred petrologically. Within this context, we examined the results of the SOM analysis to determine whether the hydrothermal alteration has resulted in the formation, modification, or destruction of soluble organic molecules and to elucidate the relationship between IOM and SOM during the alteration.

MCAs dominate the water extracts of the Tagish Lake meteorite. MCAs, such as formic and acetic acids, play essential roles in biochemistry (*11, 27, 28*); higher homologs are the fatty acids that self-assemble into membrane-bound vesicles in meteorite extracts and are the possible precursors of cell membranes (*29*). We identified 11 MCAs in all specimens, including most of the members of the homologous series of linear, saturated MCAs from C_1 to C_{10}. One or two branched isomers were detected in all specimens with the exception of 5b, in which 17 branched isomers were detected, in addition to the 11 linear MCAs. Numerous alkyl-substituted phenols were also found exclusively in 5b. Although, as in previous studies, $\delta^{13}C$ values are generally consistent with terrestrial values, these MCA hydrogen isotopic compositions are D-enriched, consistent with an extraterrestrial origin (*2*): As measured in 5b, δD (acetic), 247‰; δD (formic/propanoic), 708‰; δD (butanoic), 562‰; δD (isopentanoic), 697‰ (*13*). The observed concentrations of these low-molecular-weight MCAs are unusually high relative to those seen in other studies of carbonaceous chondrites [including Tagish Lake (*18*)], ranging from 42 to 250 parts per million (ppm) for formic and acetic acid (*13*). We attribute these large concentrations to the preservation of the meteorite below 0°C since its recovery, which has minimized the loss of volatile organics, such as formic acid, as well as the specifics of the analytical methods (*13*). In nearly all specimens, the concentrations of the straight-chain MCAs decrease in a logarithmic manner as the C number increases, with the exception of 5b, in which the acetic acid concentration exceeds that of formic acid. The $\delta^{13}C$ values of MCAs differ among the specimens (Fig. 2). All specimens have common $\delta^{13}C$ ~ –20‰ for formic acid, and higher homologs approach a constant value of ~ –5‰ (average nonanoic acid = –26 ± 2‰) with increasing C number. The largest differences are observed in acetic acid, which ranges from +8‰ (11h) to –36‰ (5b). Of particular note is specimen 11h, which shows a decrease in $\delta^{13}C$ with increasing C number (Fig. 2).

The differences in MCAs among the Tagish Lake specimens may be explained by differing degrees of parent body modification. With the exception of formic acid, specimens 5b and 11h contain the highest concentrations of MCAs, 2 to 10 times greater than concentrations in 11i and 11v (*13*), attributable to loss or destruction of these water-soluble compounds during progressive parent body alteration. The high proportion of branched isomers in specimen 5b suggests that it preserves a more primary suite of compounds

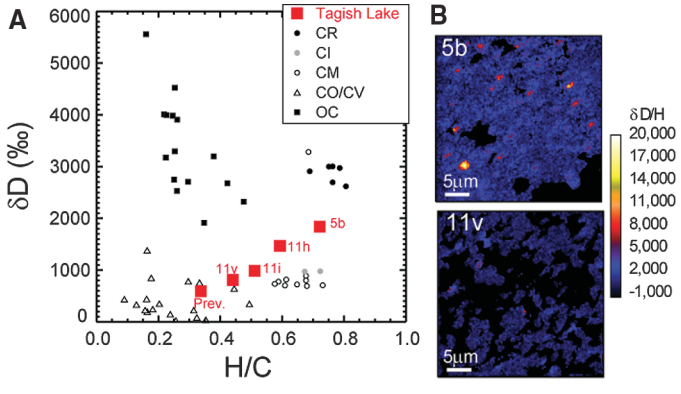

Fig. 1. (A) Plot of H/C, a measure of the degree of aliphatic character, against H isotopic composition for the Tagish Lake specimens, including data on the Tagish Lake meteorite from previous work (*8*). Also shown are representative data from other chondrite groups after (*8*), including ordinary chondrites (OC). For reference, the H/C value of an aliphatic molecule with infinite chain length is 2; aromatic organic matter has a maximum H/C = 1 (benzene), and approaches low values (~0.1) as the number of fused aromatic rings approaches infinity. **(B)** Maps of δD/H values of IOM separates from Tagish Lake specimens 5b and 11v, derived from H and D raster ion images acquired with a Cameca NanoSIMS 50L ion microprobe.

(*2*). The MCA pattern for 11h shows a trend of decreasing $\delta^{13}C$ with increasing C number, comparable to results for Murchison (*30*). Whereas this trend has been attributed to the preservation of the signature of kinetically controlled C addition in MCA synthesis, which takes place in cold, interstellar, or nebular environments (*31*), our results, which suggest that specimen 11h is more altered than 5b, imply that such a pattern may be a secondary signature. One possible explanation for the pattern in this case is the preferential exchange of MCA carboxyl C with inorganic C during hydrothermal processing, analogous to the process that occurs in oil-prone source rocks on Earth (*32*). In the Tagish Lake meteorite, the presence of carbonate $\delta^{13}C \sim 67‰$ (*17*) may provide a source of isotopically enriched carbonate for such exchange. Notably, formic acid concentration and C isotopic composition remain relatively constant among the specimens (*13*), which suggests that they are relatively unaffected by aqueous alteration (*10*) and may be inherited from preaccretionary material.

Amino acid concentrations and enantiomeric excesses in the Tagish Lake specimens provide further evidence of the influence of parent body aqueous alteration on SOM. We determined the distribution and enantiomeric abundances of the one- to six-C aliphatic amino acids found in extracts of specimens, 5b, 11h, and 11i by ultra-performance liquid chromatography fluorescence detection and time-of-flight mass spectrometry (*33*). We measured stable C isotope analyses of the most abundant amino acids in 11h with gas chromatography coupled with quadrupole mass spectrometry and isotope ratio mass spectrometry. The total abundances of amino acids decrease in the order 11h (5.6 ppm) > 5b (0.9 ppm) > 11i (0.04 ppm). The abundances of many amino acids in 11i were below the analytical detection limit (<1 part per billion), which is consistent with a much higher degree of alteration experienced by 11i as compared to 11h and 5b. The abundance of the nonprotein amino acid α-aminoisobutyric acid in specimen 11h was 0.2 ppm, approximately 200 times higher than previously measured in two different Tagish Lake meteorite samples (*18*, *19*). Glycine is the most abundant amino acid in 11h and has a C isotope value of $\delta^{13}C = +19‰$, which falls well outside the range for terrestrial organic C of −6 to −40‰ (*34*) and is consistent with an extraterrestrial origin.

The enantiomeric ratios of alanine, β-amino-*n*-butyric acid, and isovaline in 11h were racemic within uncertainties (D/L = 1), providing additional evidence of an extraterrestrial origin for these amino acids. In contrast to specimen 11h, nonracemic isovaline was detected in 5b, with an L-enantiomeric excess of ~7%, and no isovaline was identified in 11i above the detection limit. Although the mechanism of enrichment remains unclear, it has been previously shown that L-isovaline enantiomeric excesses (ee's) and the ratio of β-alanine to glycine both increase relative to the degree of aqueous alteration for many carbonaceous chondrite groups (*33*, *35*). Although the data for specimen 11i relative to 11h or 5b fit this trend (Fig. 3), in detail the sequence of alteration for 5b and 11h based on these criteria suggests that 5b is more altered than 11h, in contrast to the result from petrography and IOM. This result suggests that other factors may influence ee's and the β-alanine/glycine ratio that are apparent in the Tagish Lake meteorite. The higher ratio of β-alanine to glycine in 5b (~0.6) as compared to 11h (~0.2) may be due to enhanced production of glycine during aqueous alteration of 11h via reactions involving hydroxy acids known to be present in SOM (*36*, *37*). A study of L-isovaline ee's in Murchison specimens showed a range of ee values from 0 to 15%, roughly correlative with the abundance of hydrated minerals in the samples, indicating the role of multiple, complex, parent body synthetic processes in amino acid formation (*38*). The amino acids in Tagish Lake 11h, including ee's and overall abundance, may therefore be interpreted as reflecting a secondary pulse of amino acid formation resulting from hydrothermal alteration on the Tagish Lake parent body, which overprinted any original ee's with a racemic mixture.

Substantial heterogeneity is preserved within the Tagish Lake meteorite, especially in terms of organic matter. The correlation between differences in organic matter properties and indicators of hydrothermal alteration indicates that the processes were active after accretion onto the parent body. In this scenario, chondritic components, including D- and ^{15}N-rich IOM that is best pre-

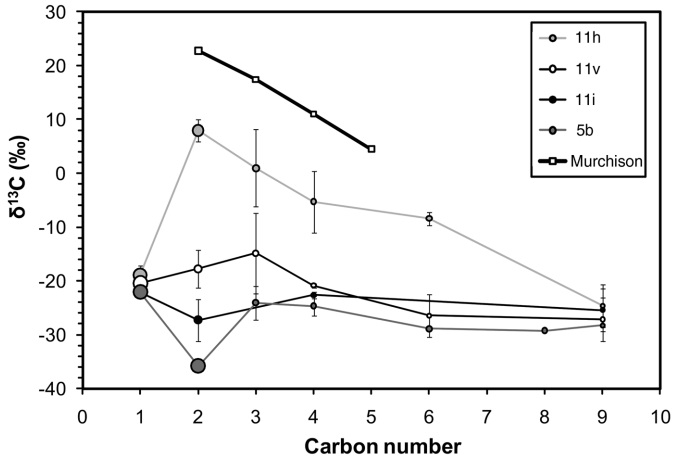

Fig. 2. C isotopic composition of monocarboxylic acids in the Tagish Lake meteorite. Uncertainties represent the standard deviation of three injections for each sample. For measurements with low amplitude (such as those of nonanoic or decanoic acid) we used a value of 4‰, which is based on the accuracy achieved for standards run with low concentrations. Also shown are the results from (*31*) for Murchison monocarboxylic acids. Symbol size reflects relative concentration (*13*).

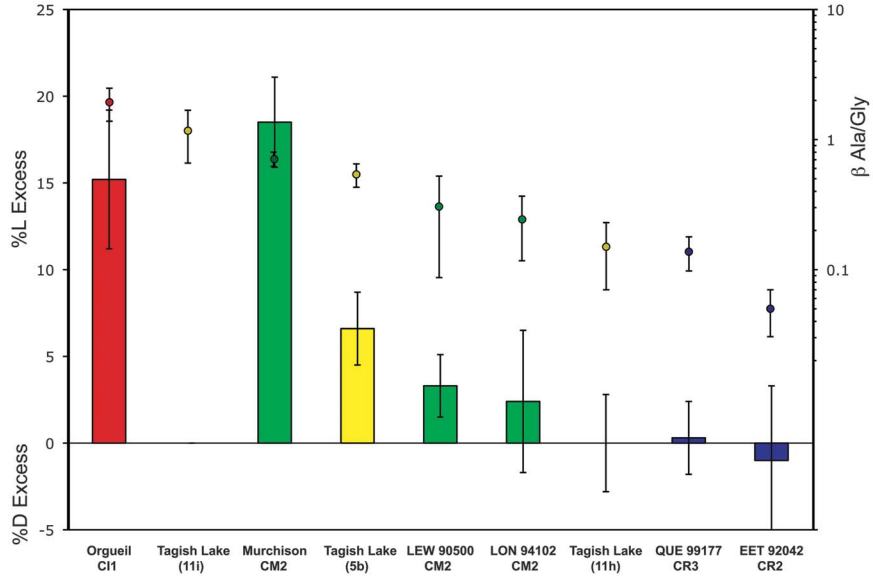

Fig. 3. L-isovaline ee's (bars) and β-alanine/glycine ratios (circles) in Tagish Lake meteorite specimens 11h, 5b, and 11i (shown in yellow), compared with results from CI (red), CM (green), and CR (blue) chondrites of differing degrees of aqueous alteration [data from (*33*)]. The percentage of L excess is defined as $L_{ee} = L\% - D\%$, with a negative value corresponding to a D excess. LEW, Lewis Cliff; LON, Lonewolf Nunataks; QUE, Queen Alexandra Range; EET, Elephant Moraine.

served in 5b, were accreted, along with (presumably) amino acid precursors. The α-amino acids were probably produced during alteration on the Tagish Lake parent body, presumably by Strecker synthesis (*37*, *39*), although other formation mechanisms for both α and other amino acids before their incorporation in the parent body have been suggested (*40*). Modest alteration may have produced light acetic acid and an initial complement of MCAs from IOM, by analogy with experiments (*11*), as well as a slight ee in isovaline, to provide the SOM characteristics observed in 5b. These components were then modified on the parent body through further hydrothermal alteration, resulting in reduction of aliphatic character and D/H in IOM, exchange of isotopically heavy C with MCA carboxyl C, production of glycine, and a fresh influx of racemic amino acids, as represented by organic matter in 11h. By analogy with MCAs, the exchange of isotopically heavy C with amino acid carboxyl C may explain the positive $\delta^{13}C$ values of amino acids in 11h (such as glycine). The increase in IOM $\delta^{13}C$ with the degree of alteration (Table 1) is consistent with the loss of isotopically lighter C, associated with aliphatics, such as MCAs in 11i and 11v. Further hydrothermal alteration resulted in further modification of IOM and decreases in overall concentration of MCAs in 11i and 11v and a nearly complete loss of amino acids in 11i. The conditions of hydrothermal alteration inferred by analogy with experiments, especially temperature (~300°C) (*10*, *11*, *25*), are at odds with the mineralogy and preservation of volatile organic compounds, which provide an upper limit of ~150°C (*23*). The Tagish Lake specimens may therefore have experienced alteration at lower temperatures than those in the experiments, with the more extensively altered samples having been subjected to longer periods of alteration, higher temperatures, and/or higher water/rock ratios (*11*).

References and Notes

1. E. R. D. Scott, A. N. Krot, in *Treatise on Geochemistry,* H. D. Holland, K. K. Turekian, Eds. (Elsevier Pergamon, Oxford, 2007), vol. 1, pp. 1–72.
2. I. Gilmour, in *Treatise on Geochemistry,* H. D. Holland, K. K. Turekian, Eds. (Elsevier Pergamon, Oxford, 2003), vol. 1, pp. 269–290.
3. O. Botta, J. L. Bada, *Surv. Geophys.* **23**, 411 (2002).
4. J. R. Cronin, S. Pizzarello, D. P. Cruikshank, in *Meteorites and the Early Solar System,* J. F. Kerridge, M. S. Matthews, Eds. (Univ. of Arizona Press, Tucson, AZ, 1988), pp. 819–857.
5. H. Busemann *et al.*, *Science* **312**, 727 (2006).
6. S. A. Sandford *et al.*, *Science* **314**, 1720 (2006).
7. J. Duprat *et al.*, *Science* **328**, 742 (2010).
8. C. M. O. D. Alexander, M. Fogel, H. Yabuta, G. D. Cody, *Geochim. Cosmochim. Acta* **71**, 4380 (2007).
9. C. F. Chyba, P. J. Thomas, L. Brookshaw, C. Sagan, *Science* **249**, 366 (1990).
10. Y. Huang, M. R. Alexandre, Y. Wang, *Earth Planet. Sci. Lett.* **259**, 517 (2007).
11. Y. Oba, H. Naraoka, *Meteorit. Planet. Sci.* **41**, 1175 (2006).
12. L. Remusat, S. Derenne, F. Robert, H. Knicker, *Geochim. Cosmochim. Acta* **69**, 3919 (2005).
13. Information on materials and methods is available as supporting material on *Science* Online.
14. Hydrothermal alteration occurred early in the history of the carbonaceous chondrite parent bodies owing to accumulation of the heat of radioactive decay, so that liquid water was transiently present and percolated through the mineral matrix. The evidence for this process is preserved in mineral alterations. Furthermore, in the interior of the parent body, the temperature and pressure can rise high enough to produce hydropyrolysis of organic material.
15. M. E. Zolensky *et al.*, *Meteorit. Planet. Sci.* **37**, 737 (2002).
16. T. Hiroi, M. E. Zolensky, C. M. Pieters, *Science* **293**, 2234 (2001).
17. M. M. Grady, A. B. Verchovsky, I. A. Franchi, I. P. Wright, C. T. Pillinger, *Meteorit. Planet. Sci.* **37**, 713 (2002).
18. S. Pizzarello *et al.*, *Science* **293**, 2236 (2001).
19. G. Kminek, O. Botta, D. P. Glavin, J. L. Bada, *Meteorit. Planet. Sci.* **37**, 697 (2002).
20. K. Nakamura-Messenger, S. Messenger, L. P. Keller, S. J. Clemett, M. E. Zolensky, *Science* **314**, 1439 (2006).
21. R. K. Herd, C. D. K. Herd, *Lunar Planet. Sci.* XXXVIII, abstr. 2347 (2007).
22. P. G. Brown *et al.*, *Science* **290**, 320 (2000).
23. A. J. Brearley, in *Treatise on Geochemistry,* H. D. Holland, K. K. Turekian, Eds. (Elsevier Pergamon, Oxford, 2003), vol. 1, pp. 247–268.
24. A. L. D. Kilcoyne *et al.*, *J. Synchrotron Radiat.* **10**, 125 (2003).
25. H. Yabuta, L. B. Williams, G. D. Cody, C. M. O. Alexander, S. Pizzarello, *Meteorit. Planet. Sci.* **42**, 37 (2007).
26. G. D. Cody, C. M. O. D. Alexander, *Geochim. Cosmochim. Acta* **69**, 1085 (2005).
27. M. C. Anguera *et al.*, *J. Biol. Chem.* **281**, 18335 (2006).
28. G. K. Smith, W. T. Mueller, L. J. Slieker, C. W. DeBrosse, S. J. Benkovic, *Biochemistry* **21**, 2870 (1982).
29. D. Deamer, J. P. Dworkin, S. A. Sandford, M. P. Bernstein, L. J. Allamandola, *Astrobiology* **2**, 371 (2002).
30. Y. S. Huang *et al.*, *Geochim. Cosmochim. Acta* **69**, 1073 (2005).
31. G. Yuen, N. Blair, D. J. Des Marais, S. Chang, *Nature* **307**, 252 (1984).
32. R. F. Dias, K. H. Freeman, M. D. Lewan, S. G. Franks, *Geochim. Cosmochim. Acta* **66**, 2755 (2002).
33. D. P. Glavin, J. P. Dworkin, *Proc. Natl. Acad. Sci. U.S.A.* **106**, 5487 (2009).
34. R. Bowen, in *Isotopes in the Earth Sciences*, R. Bowen, Ed. (Kluwer, New York, 1988), pp. 452–469.
35. D. P. Glavin, M. P. Callahan, J. P. Dworkin, J. E. Elsila, *Meteorit. Planet. Sci.* **45**, 1948 (2010).
36. J. R. Cronin, S. Pizzarello, S. Epstein, R. V. Krishnamurthy, *Geochim. Cosmochim. Acta* **57**, 4745 (1993).
37. E. T. Peltzer, J. L. Bada, G. Schlesinger, S. L. Miller, *Adv. Space Sci.* **4**, 69 (1984).
38. S. Pizzarello, M. Zolensky, K. A. Turk, *Geochim. Cosmochim. Acta* **67**, 1589 (2003).
39. E. T. Peltzer, J. L. Bada, *Nature* **272**, 443 (1978).
40. J. E. Elsila, J. P. Dworkin, M. P. Bernstein, M. P. Martin, S. A. Sandford, *Astrophys. J.* **660**, 911 (2007).
41. Where given, the errors are half the difference (standard error of the mean) between the compositions of two residues prepared from two separate aliquots of each specimen. Typically, the differences in elemental ratios and isotopic compositions are larger than the intrinsic measurement precisions. Where only one measurement was made, the uncertainties of the other samples are a guide to the likely uncertainties.

Acknowledgments: Funding for this study was provided by the Natural Sciences and Engineering Research Council of Canada, Alberta Innovates, NASA (Astrobiology, including Carnegie Institution Astrobiology and the Goddard Center for Astrobiology; Origins of Solar Systems; Cosmochemistry and Postdoctoral Programs), the U.S. Office of Naval Research, the CIW, Grant MacEwan University, and the Carnegie Institution of Canada. The Canadian Institute for Advanced Research is thanked for hosting workshops that facilitated work on the MCAs. J. Kirby assisted with MCA analysis. R. Bowden carried out bulk IOM analyses. XANES data were acquired on the Scanning Transmission X-ray Microscope at beamline 5.3.2.2 of the Advanced Light Source, which is supported by the Director of the Office of Science, U.S. Department of Energy, under contract no. DE-AC02-05CH11231, and by a W.M. Keck Foundation grant to the CIW. Three anonymous reviewers are thanked for constructive comments that improved the manuscript.

Supporting Online Material

www.sciencemag.org/cgi/content/full/332/6035/1304/DC1
Materials and Methods
Figs. S1 to S5
Tables S1 to S4
References (*42*–*50*)

25 January 2011; accepted 6 May 2011
10.1126/science.1203290

Activation of Visual Pigments by Light and Heat

Dong-Gen Luo,[1,3]* Wendy W. S. Yue,[1,3,4] Petri Ala-Laurila,[5,6] King-Wai Yau[1,2,3]*

Vision begins with photoisomerization of visual pigments. Thermal energy can complement photon energy to drive photoisomerization, but it also triggers spontaneous pigment activation as noise that interferes with light detection. For half a century, the mechanism underlying this dark noise has remained controversial. We report here a quantitative relation between a pigment's photoactivation energy and its peak-absorption wavelength, λ_{max}. Using this relation and assuming that pigment activations by light and heat go through the same ground-state isomerization energy barrier, we can predict the relative noise of diverse pigments with multi–vibrational-mode thermal statistics. The agreement between predictions and our measurements strongly suggests that pigment noise arises from canonical isomerization. The predicted high noise for pigments with λ_{max} in the infrared presumably explains why they apparently do not exist in nature.

Our visual system has an extremely high sensitivity to light under dark-adapted conditions (*1*). This feat requires a photo-transduction mechanism with high amplification (*2*) and a thermally quiet visual pigment for minimizing noise. Thermal energy is a double-edged

www.sciencemag.org/cgi/content/full/332/6035/1304/DC1

Supporting Online Material for

Origin and Evolution of Prebiotic Organic Matter As Inferred from the Tagish Lake Meteorite

Christopher D. K. Herd,* Alexandra Blinova, Danielle N. Simkus, Yongsong Huang, Rafael Tarozo, Conel M. O'D. Alexander, Frank Gyngard, Larry R. Nittler, George D. Cody, Marilyn L. Fogel, Yoko Kebukawa, A. L. D. Kilcoyne, Robert W. Hilts, Greg F. Slater, Daniel P. Glavin, Jason P. Dworkin, Michael P. Callahan, Jamie E. Elsila, Bradley T. De Gregorio, Rhonda M. Stroud

*To whom correspondence should be addressed. E-mail: herd@ualberta.ca

Published 10 June 2011, *Science* **332**, 1304 (2011)
DOI: 10.1126/science.1203290

This PDF file includes:

Supplemental Online Material

The Fall and Specimen Nomenclature

The Tagish Lake meteorite entered the upper atmosphere as an object (meteoroid) ~4 m in diameter (*22*). As with other meteorite falls, the Tagish Lake meteoroid broke up into fragments due to pressure shock, and outer surfaces were heated due to atmospheric friction. However, because the transit through the atmosphere is only a few seconds in duration, the high temperature of the surface does not penetrate beyond a depth of ~ 1-2 mm, thus preserving the internal composition of the meteorites - including organics - against pyrolysis.

Individual stones of the Tagish Lake meteorite were collected from the frozen surface of the lake on January 25 and 26, 2000. Some of these specimens were then sent to NASA Johnson Space Center in Houston, Texas, for preliminary investigation, and the rest remained with the finder in Atlin, British Columbia. In August 2000 the specimens in Houston and Atlin were documented by R.K. Herd and a report prepared with an alphanumeric list of specimens (1 through 11, including lettered sub-specimens) with weights and photographs. This listing forms the basis of the documentation during acquisition of the specimens in 2006, and the nomenclature for the pristine Tagish Lake specimens. Previous work on Tagish Lake IOM as shown in Figure 1 and Table 1, after (*8*) was carried out on material collected during spring thaw in April 2000. The petrographic context of this material, obtained from A.R. Hildebrand, is unknown.

SOM extraction and analysis methods

Monocarboxylic Acid Analysis: Concentrations

In a typical extraction, a ~0.70 g-subsample of the specimen was taken from storage at -30^{o}C and added expeditiously to a 50 mL round-bottomed flask containing 20 mL of ultrapure deionized water. The flask and its contents were allowed to achieve ambient temperature, the meteorite material was crushed into a fine powder with a glass rod and the resulting black suspension was heated at reflux (100^{o}C) for 6 h. The "cooked" suspension was then cooled, filtered through glass wool that had been scrupulously washed with distilled, deionized water, and the pH of the colorless filtrate increased to ~11 via the addition of 4 drops of ultrapure 6 M NaOH(aq) (prepared from Sigma-Aldrich Traceselect sodium hydroxide monohydrate and ultrapure water). This step converts all carboxylic acids present into their corresponding, non-volatile carboxylate salts. The volume of the filtrate was then reduced to ~1 mL on a rotary evaporator operating at 75^{o}C. In order to regenerate the acids, the pH of the concentrate was

pushed below 2 by the addition of 8 drops of ultrapure 6 M HCl(aq)(prepared from Fisher Gold Label ultrapure concentrated HCl(aq)and ultrapure water). A subsequently prepared procedural blank was found to contain trace amounts (less than 1 ppm) of formic and acetic acid. The carboxylic acids in the concentrated extracts were determined by using solid phase micro extraction (SPME) in combination with an Agilent 6890N gas chromatograph (GC) equipped with a 5973 inert mass selective detector (MS). The column used was 30m, 0.25 µm and 0.25 mm id Nukol™, with helium flow maintained at 1.1 mL/min. The GC injection port was held at 210°C, splitless. The GC oven was programmed at 35°C hold for 1 minute, ramp at 25°C/minute to 135°C, ramp at 1.5°C/minute to 185°C and hold for 10 minutes. A Carbowax–Polyethylene Glycol (PEG) coated fibre, 23 gauge, 1 cm, 60 µm film thickness was used to extract the carboxylic acids from the samples and standards. All samples and standards were in a total volume of 1.5 mL and treated in the same manner. The acids were adsorbed onto the fibre for 15 minutes with stirring and then desorbed into the GC injection port for 10 minutes. The samples were quantified via external calibration. A mixed standard was prepared containing all the linear monocarboxylic acids from C_1-C_{10}. Calibration curves were prepared for each carboxylic acid using five concentration levels. For samples 11h and 5b, each compound was quantified against the corresponding calibration curve using single ion extraction and the total µg on the fibre was calculated. A fibre blank was run and all samples were injected at least in duplicate (11h, 11i and 11v were injected 3x while 5b was injected 2x). The concentrations for the formic and acetic acid in samples 11v and 11i were quantified by referring the peak areas to standard curves using six concentration levels. As a representative example, we have provided the standard curve constructed for formic acid in Figure S1. The concentration for each of the longer chain homologues found in samples 11v and 11i was estimated by comparison of the peak area for the acid in the meteorite extract to a single standard solution for the acid run under the same conditions. The monocarboxylic acid concentrations derived from these studies are collected in Tables S1-4.

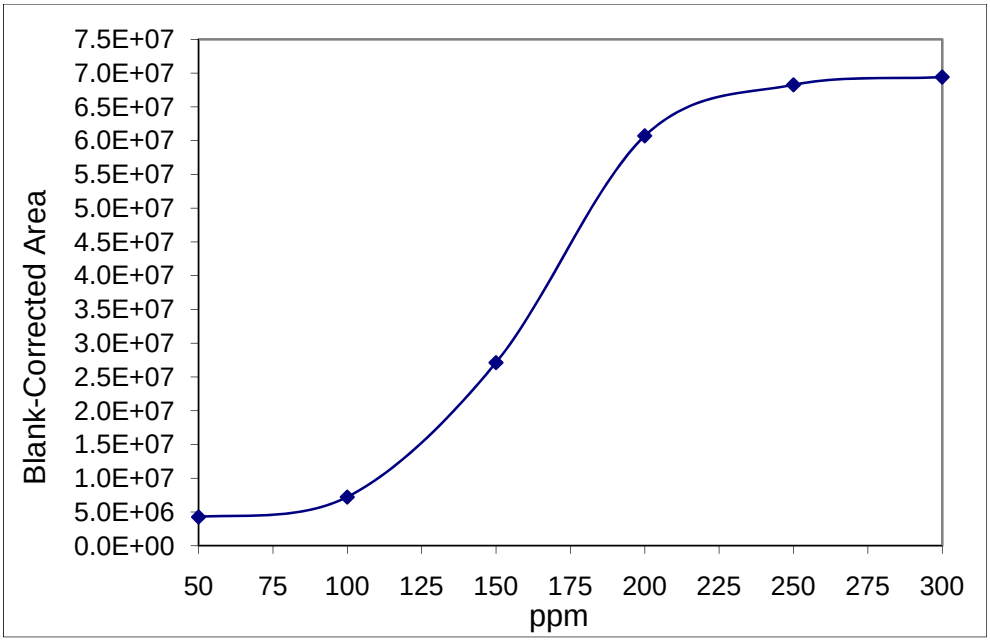

Figure S1. Blank-corrected Formic Acid Concentration Response.

At least eleven monocarboxylic acids were positively identified in the aqueous extract of 11v including most of the members of the homologous series of linear, saturated monocarboxylic acids from C_1 to C_{10}, two branched, saturated monocarboxylic acids, an unsaturated, branched monocarboxylic acid and the aromatic carboxylic acids benzoic acid and 4-methylbenzoic acid. It is noteworthy that the concentrations of the straight-chain carboxylic acids decrease in a logarithmic manner as the carbon number grows. The chromatograms for the water extracts of 11i and 11h are closely comparable to that for 11v (See Tables S2 and S3). In both the 11i and 11v extracts, carboxylic acids are again the dominant compounds, and, as with 11v, the straight-chain carboxylic acid abundances fall logarithmically with increasing chain length. Also, as was found for the 11v extract, the majority of the carboxylic acids that are present in the chromatograms of 11i and 11h are linear isomers. In fact, only two branched carboxylic acids were found in the extract for 11v, while the 11i and 11h extracts each contained just one branched isomer. The trace for the extract of 5b is markedly different from the other three. First of all, there are more branched than linear monocarboxylic acids in the trace for 5b (17 branched versus 11 linear MCAs). In fact, owing to the large number of different types of branched isomers, it would appear that the abundances for the branched and linear carboxylic acids are comparable, which is not the case for the other three specimens, which have linear carboxylic acids in much greater abundances. Finally,

examples of alkyl-substituted benzoic acids are also present in all four of the extracts (i.e., 11v, 11i, 11h and 5b).

Monocarboxylic Acids: Compound-Specific Carbon Isotopes

Carbon isotope analysis of the monocarboxylic acids in the four specimens was accomplished by using the SPME methodology with GCIRMS, in the manner of (*30*). Individual acids were separated by GC(Agilent 6890N), completely burned with molecular oxygen, and the combustion product, CO_2 gas, was analyzed in a Finnigan DeltaPlus XP isotope ratio mass spectrometer in the School of Geography and Earth Sciences, McMaster University. The GC conditions used for the GCIRMS analyses were the same as those used initially to obtain the standard GC-MS spectrum of the sample, viz. 10 min desorption in the GC injection port at 210°C, followed by temperature programming from 35 to 135^{o}C @ 25^{o}C/min-185^{o}C @ 1.5^{o}C/min and hold for 10 min. The δ^{13}C values for the monocarboxylic acids are quoted relative to the VPDB standard. For samples 11v, 11h and 5b, $\delta\ ^{13}$C values were obtained for most of the members of the homologous series of linear carboxylic acids from C1 to C10. By contrast, for 11i, $\delta\ ^{13}$C values were obtained for just four from the C_1-C_{10} linear monocarboxylic acid series as these were the only acids for which concentrations were sufficiently high for C isotopic analysis. Results are given in Tables S1-S4.

Monocarboxylic Acids: Compound-Specific Hydrogen Isotopes

Hydrogen isotope analyses of the individual monocarboxylic acids in 5b were performed by combining SPME (polyethylene glycol fiber) with GCIRMS(Nukol column), following the method optimized by (*30*). The carboxylic acids were separated on 30 m x 0.25 mm x 0.25µm NUKOL column inside an HP 6890 GC at Brown University. The separated acids were then converted to H_2 in a pyrolysis furnace. Because the concentrations of the indigenous acids were very low for GCIRMS, a bath of dry ice and isopropanol was applied to the outside of the column just below the injector port as a means of minimizing loss of volatile acids. Also, in order to ensure that as many acids as possible produced peaks with acceptable signal-to-noise ratios, three consecutive SPME sorption desorption cycles were performed on aqueous extract prior to transfer into the column. The sample was analyzed in duplicate. The GC conditions used for the Hydrogen Isotope GCIRMS analyses were the same as those described above for the ^{13}C GCIRMS analyses. The δ D values for the monocarboxylic are quoted with respect to the VSMOW standard. Not surprisingly, owing to the low sensitivity of the deuterium isotope, we were only able to obtain δD values for seven (two branched and five linear) of the 34 identified monocarboxylic acids in the aqueous extract of 5b. Sample size and MCA concentrations limited analysis of MCA δ D to sample 5b.

Results from specimen 5b are given in Table S1. It should also be mentioned here that formic and propanoic acid coelute on the Nukol column that was used for the GCIRMS determination of δD values. The 708 ‰ value δ D value found for the amalgamated peak is therefore the arithmetic combination of the two individual δ D values for these acids. Owing to the nature of this technique, the individual δ D values cannot be extracted from the combined value.

Table S1: Selected Monocarboxylic Acids in Tagish Lake specimen 5b

Compound	Conc. (ppm)	δ13C ± S.D. (per mil)	δ D ± S.D. (per mil)	Compound Number	Relative GC Response Factors
formic acid*	178	-22 ± 1	708 ± 20	1	1
acetic acid	250	-36 ± 1	247 ± 5	2	2.5
propanoic acid*	8.2	-24 ± 3	708 ± 20	3	5.7
isobutanoic acid	< 5	**	493 ± 12	4	*
butanoic acid	5.7	-25 ± 2	562 ± 1	5	11
isopentanoic acid	**	**	697 ± 2	6	*
hexanoic acid	4.5	-29 ± 1	**	7	55
octanoic acid	1.6	-29 ± 1	**	8	195
nonanoic acid	0.62	-28 ± 5	**	9	281
decanoic acid	0.04	-24 ± 5	**	10	395
2-methypropanoic acid	**	**	**	12	**
2-methylbutanoic acid	**	**	**	13	**
3-methylbutanoic acid	**	**	**	14	**
3,3-dimethylbutanoic acid	**	**	**	15	**
2,2-dimethylbutanoic acid	**	**	**	16	**
2(E)-butenoic acid	**	**	**	17	**
2-ethylpentanoic acid	**	**	**	18	**
2-methylpentanoic acid	**	**	**	19	**
2,2-dimethylpentanoic acid	**	**	**	20	**
3-methylpentanoic acid	**	**	**	21	**
2(Z)-butenoic acid	**	**	**	22	**
4-methylpentanoic acid	**	**	**	23	**
2-ethyl, 2-methylpentanoic acid	**	**	**	24	**
2-methylhexanoic acid	**	**	**	25	**
3-methylhexanoic acid	**	**	**	26	**
4-methylhexanoic acid	**	**	**	27	**
2-ethylhexanoic acid	**	**	**	28	**
heptanoic acid	**	**	**	29	**

2-methylheptanoic acid	**	**	**	30	**
3-methylheptanoic acid	**	**	**	31	**
benzoic acid	**	**	**	32	**
2-methylbenzoic acid	**	**	**	33	**
3-methylbenzoic acid	**	**	**	34	**
4-methylbenzoic acid	**	**	**	35	**
dimethylbenzoic acid	**	**	**	36	**
benzeneacetic acid	**	**	**	37	**
ethylbenzoic acid	**	**	**	38	**
dimethylbenzoic acid	**	**	**	39	**

* = formic acid and propanoic acid coelute on the IRMS column

** = not determined

Total abundance for those MCAs in 5b whose concentrations were estimated via comparison to external standards: ca. 454 ppm.

Table S2: Selected Monocarboxylic Acids in Tagish Lake specimen 11h

Compound	Conc. (ppm)	$\delta^{13}C \pm$ S.D. (‰)	Number	Relative GC Response Factors
formic acid	155.5	-19 ± 2	1	1
acetic acid	110.4	8 ± 2	2	2.5
propanoic acid	26.1	1 ± 7	3	5.7
isobutanoic acid	*	*	4	*
butanoic acid	6	-5 ± 6	5	11
hexanoic acid	1.3	*	6	55
octanoic acid	0.8	*	7	195
nonanoic acid	0.2	-25 ± 5	8	281
decanoic acid	0.1	-2 ± 5	9	395
benzoic acid	*	*	10	*

* = not determined

Total abundance for those MCAs in 11h whose concentrations were estimated via comparison to external standards: ca. 301 ppm.

Table S3: Selected Monocarboxylic Acids in Tagish Lake specimen 11i

Compound	Conc. (ppm)	$\delta^{13}C \pm$ S.D. (‰)	Number	Relative GC response factors
formic acid	120	-22 ± 1	1	1
acetic acid	42	-27 ± 4	2	2.5
propanoic acid	2	*	3	5.7
isobutanoic acid	*	*	4	*
butanoic acid	0.6	-23 ± 1	5	11
hexanoic acid	0.4	*	6	55
octanoic acid	0.1	*	7	195
nonanoic acid	0.4	-25 ± 5	8	281

decanoic acid	< 0.01	*	9	395
benzoic acid	*	*	10	*
4-methylbenzoic acid	*	*	11	*

* = not determined
Total abundance for those MCAs in 11i whose concentrations were estimated via comparison to external standards: ca. 166 ppm

Table S4: Selected Monocarboxylic Acids in Tagish Lake specimen 11v

Compound	Conc.(ppm)	$\delta^{13}C \pm$ S.D. (‰)	Number	Relative GC Response Factors
formic acid	200	-21 ± 2	1	1
acetic acid	46	-18 ± 4	2	2.5
propanoic acid	3.5	-15 ± 8	3	5.7
isobutanoic acid	*	*	4	*
butanoic acid	0.8	-21 ± 1	5	11
isopentanoic acid	*	*	6	*
hexanoic acid	0.4	-27 ± 5	7	55
octanoic acid	0.08	*	8	195
nonanoic acid	0.2	-27 ± 4	9	281
decanoic acid	< 0.01	-17 ± 4	10	395
benzoic acid	*	*	11	*
3-methylbenzoic acid	*	*	12	*

* = not determined
Total abundance for all linear monocarboxylic acids in 11v: ca. 251 ppm.

Amino acids: Liquid Chromatography with UV Fluorescence Detection and Time of Flight Mass Spectrometry

We investigated the abundance of amino acids, as well as their enantiomeric composition, in dichloromethane extracts from the Tagish Lake meteorite fragments 11h, 11i, and 5b using ultra performance liquid chromatography with simultaneous UV fluorescence and time of flight-mass spectrometry detection (UPLC-FD/ToF-MS). The UPLC-FD/ToF-MS analyses were identical to those described in (*35*). The Tagish Lake extracts were obtained by heating ~2 to 3 grams of each powdered meteorite fragment in ultrapure water for 6 hours followed by rotoevaporation of the water and then re-dissolution of the residue in dichloromethane (DCM). For the amino acid analyses, we received a fraction of the dried residues of the DCM extracts corresponding to 50% splits for 11h and 5b, and a 75% split for 11i. The DCM extracts were redissolved in 5 ml of Millipore Direct Q3 UV (18.2 MΩ, < 5 ppb total organic carbon) ultrapure water. A procedural blank was also carried through the same extraction

and analytical procedures as the Tagish Lake meteorite samples. Half of each water extract was dried in a separate glass test tube and subjected to a 6 M HCl acid vapor hydrolysis procedure at 150°C for 3 h to determine total hydrolysable amino acid content (*42*). The acid-hydrolyzed, hot-water extracts were desalted by using cation-exchange resin (AG50W-X8, 100-200 mesh, hydrogen form, BIO-RAD), and the amino acids recovered by elution with 2 M NH_4OH (prepared from Millipore water and NH_3(g) (AirProducts, *in vacuo*). The non-hydrolyzed extracts of the meteorite samples were taken through the identical desalting procedure in parallel with the acid-hydrolyzed extracts. After desalting, the amino acids in the NH_4OH eluates were dried under vacuum to remove excess ammonia; the residues were then re-dissolved in 100 μL of Millipore water, transferred to sterile microcentrifuge tubes, and stored at -20°C prior to analysis.

Prior to analysis, 10 μL of each meteorite extract, procedural blank, or standard was added to 10 μL of 0.1 M sodium borate buffer at room temperature and then derivatized by adding 5 μL of *o*-phthaldialdehyde/*N*-acetyl-L-cysteine (OPA/NAC). The OPA/NAC reaction was quenched after 1 or 15 minutes with 75 μL of 0.1 M aqueous hydrazine, and 25 μL of the solution was immediately injected into a Waters ACQUITY UPLC with a fluorescence detector and Waters LCT Premier time-of-flight mass spectrometer using positive electrospray ionization. The details of the ToF-MS settings and the amino acid quantification methods used, and the range of linear response for these analyses are described elsewhere (*35*). The remaining derivatized sample (and a parallel derivatized standard) was stored in a -86°C freezer for repeat analyses. We have found through monitoring standards that OPA/NAC amino acid derivatives are stable for up to 1 week at -86°C without significant degradation. Each derivatized sample was analyzed using our standard tandem LC column conditions for initial two- to six-carbon (C_2 – C_6) amino acid separation and characterization (*35*). The first column was a Waters BEH C18 column (2.1 x 50 mm, 1.7-μm bead) followed by a second Waters BEH Phenyl-Hexyl column (2.1 x 150 mm, 1.7-μm bead). The conditions for separation of the OPA/NAC amino acid derivatives at 30ºC were as follows: flow rate, 150 μL/min; solvent A (50 mM ammonium formate, 8% methanol, pH 8.0); solvent B (methanol); gradient, time in minutes (%B): 0 (0), 35 (55), 45 (100). The following day a different gradient using the same columns and buffers optimized specifically for the separation of the five-carbon (C_5) amino acids was used to analyze the same derivatized extract on the same columns (*33*).

Amino acid abundances and their enantiomeric ratios in the meteorite extracts were determined by comparison of the peak areas generated from the UV fluorescence detector and ToF-MS of the

OPA/NAC amino acid derivatives to the corresponding peak areas of standards under the same chromatographic conditions on the same day.

Amino Acids: Gas Chromatography Isotope Ratio Mass Spectrometry

The hydrolyzed and unhydrolyzed extracts of sample 11h were combined for carbon isotopic analysis of bound and free amino acids by gas chromatography coupled with mass spectrometry and isotope ratio mass spectrometry (GC-MS/IRMS). The hydrolyzed and unhydrolyzed procedural blanks were also combined. Both the sample 11h and the procedural blank combined extracts were dried under vacuum using a LabConco CentriVap centrifugal concentrator. Samples were esterified with isopropanol and the isopropyl esters reacted with trifluoroacetic anhydride (TFAA) using established methods (e.g., *43*). Derivatized samples were dissolved in 5 µL of ethyl acetate (Fisher Chemical, Optima Grade).

The $\delta^{13}C$ of the TFAA-isopropanol derivatized samples were analyzed by GC-MS/IRMS, which provides compound-specific structural and stable isotopic information from a single sample injection. The GC-MS/IRMS instrument consists of a Thermo Trace GC whose output is split, with approximately 10% directed into a Thermo DSQII electron-impact quadrupole mass spectrometer that provides mass and structural information for each eluting peak. The remaining ~90% passes through a Thermo GC-C III interface, where eluting amino acids are oxidized and reduced to form CO_2 and N_2. These gases are passed into a Thermo MAT 253 isotope ratio mass spectrometer (IRMS) for stable isotopic measurement.

Derivatized extracts were injected in 1 µL aliquots into the GC, which was outfitted with a 5-m base-deactivated fused silica guard column (Restek, 0.25 mm ID) and four 25-m Chirasil L-Val columns (Varian, 0.25 mm ID) connected in series using Press-Tight connectors (Restek), and the following program was used: initial oven temperature was 50 °C, ramped at 10 °C/min to 85 °C, ramped at 2 °C/min to 120 °C, ramped at 4 °C/min to 200 °C, and held at 200 °C for 10 min. Six pulses of CO_2 ($\delta^{13}C$ = -24.234) that had been precalibrated against commercial reference gases (Oztech Corporation) were injected into the IRMS for computation of the $\delta^{13}C$ or $\delta^{15}N$ values of the eluting compounds. Analysis of the MAT 253 data was performed with Thermo Isodat 2.5 software.

Stock solutions of the amino acids of interest were combined to make a standard mixture that was carried through the derivatization process and run daily on the GC-MS/IRMS. A stock solution of L-

alanine with a known $\delta^{13}C$ value (-23.33‰, IsoAnalytical) was also derivatized and injected daily for calibration purposes. The individual, underivatized stock solutions or solid pure standards were also analyzed on a Costech ECS 4010 combustion elemental analyzer (EA) connected to the MAT 253 IRMS; this was necessary to correct for the carbon added during derivatization. The final $\delta^{13}C$ values of the amino acids in the samples and their precision were calculated as described elsewhere (*43-44*).

IOM Extraction and Preparation Method

The IOM residues were prepared and analyzed using the same methods as described in (*8*). The new residues were prepared using the CsF-HF technique in which crushed samples (<106 μm) are first leached with 2N HCl, followed by rinsing with milliQ water and dioxane, and then shaken in the presence of two immiscible liquids, a CsF-HF solution (1.6-17 g/cc) and dioxane. When liberated from its mineral matrix, the IOM collects at the interface of the CsF-HF solution and the dioxane, while the denser minerals sink to the bottom. After centrifugation, the IOM is pipetted off and rinsed with 2N HCl, milliQ water and then dioxane, before being dried down at <30-50°C. There was no specific attempt to remove soluble organic material. However, the repeated washing with aqueous solutions and dioxane should have effectively removed most soluble organic compounds known to be present in chondrites.

Small amounts of IOM from samples 5b and 11v were embedded in S and sliced with a diamond knife in an ultramicrotome (*45*). Relatively thick slices (>500 nm) were deposited onto cleaned Au foils for secondary ion mass spectrometry (SIMS) analysis and thinner slices (~100 nm) were deposited onto transmission electron microscopy (TEM) grids with SiO films for both conventional and scanning (STEM) TEM analysis. Subsequent heating to 60 °C for 24 hours or 70 °C for 4 hours sublimated the S, leaving the IOM slices intact.

IOM: Elemental and isotopic analyses

Elemental and isotopic analyses were made with a Finnigan MAT Delta^{plus}XL mass spectrometer at the Carnegie Institution of Washington. Sample gases were introduced into the mass spectrometer via a molecular sieve gas chromatographic (GC) column (*46-47*) connected to either: a CE Instruments NA 2500 series elemental analyzer (EA) for C and N analyses, or a Thermo Finnigan thermal conversion elemental analyzer (TC/EA) for H and O analyses. For all analyses internal working gas standards were analyzed with every sample, and external standards were analyzed at regular intervals to monitor the accuracy of the measured isotopic ratios and elemental compositions. A H_3^+ correction applied to the H

measurements was determined periodically throughout the day. Typical sample sizes were 0.2-0.4 mg. The only difference with the study of (*8*) was the use for the H and O analyses of a He-flushed autosampler to reduce the amount of water adsorbed from the atmosphere.

In addition to the analysis of the new samples, the H abundances and isotopic compositions of a number of previously analyzed residues with low H/C ratios were remeasured. The aim of this was to use the He-flushed autosampler to determine whether any of the previous analyses were significantly influenced by adsorbed water.

The measurement precision for elemental abundances is typically of the order 1-3 % of the reported values. Because C and N are measured in the same samples, the precision of measured N/C ratios is typically about 1 % of the reported values. The precision of C and N isotope measurements are generally 0.1-0.3 ‰, while for O it is typically 0.3-0.5 ‰. The precision of the H isotope measurements are more difficult to assess because it decreases with increasing D enrichment, and because there is a small memory effect associated with the measurements. Sample heterogeneity is also a potential source of uncertainty in all the measurements. Hence, uncertainties are only given for samples for which two or more measurements were made and they provide the best estimates of the likely uncertainties in the precision of the single measurements.

IOM: ^{1}H and ^{13}C Solid State NMR analyses

All solid state NMR analyses were performed at the W. M. Keck Solid State NMR facility at the Geophysical Laboratory that accommodates a Varian-Chemagnetics Infinity 300 solid NMR that employs a 7.05 Tesla superconducting solenoid permanent magnet. The ^{13}C solid state NMR experiments employed double resonance probe with a Magic Angle Spinning (MAS) probe head. Sample rotors are composed of zirconia oxide and are 5 mm diameter, MAS frequency was 12 KHz. Due the fact that the sample quantities are low (15-25 mg) ^{1}H to ^{13}C cross polarization was performed using pulse amplitude ramping on the ^{13}C channel to maximize signal and where the experiment was tuned with organic solid standards to ensure that the polarization transfer spectrum is identical to that obtained via direct polarization. The ^{1}H solid state NMR experiments employed a double resonance MAS probe with fast MAS capility. MAS frequencies of 21 KHz were sufficient to resolve the aromatic and aliphatic Hs. A multipulse background suppression pulse sequence is used to suppress signal from protonated solids outside of the RF coil. Results are shown in Figure S2.

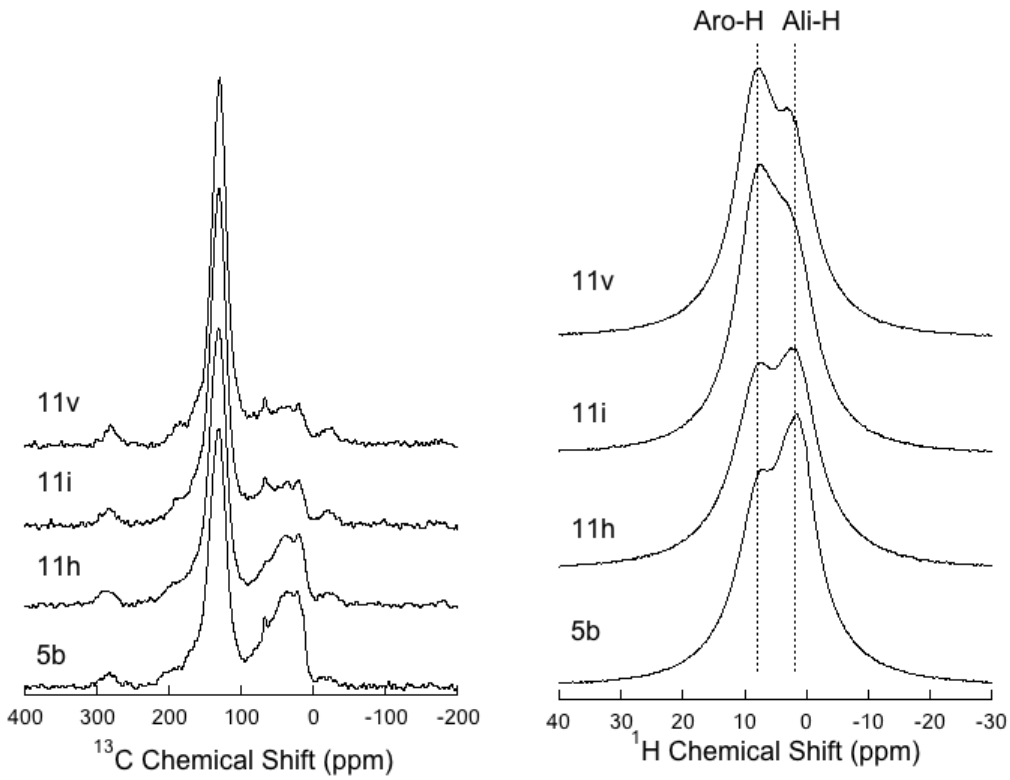

Figure S2: Left: ^{13}C VACPMAS solid state NMR spectra of Tagish Lake specimens 5b, 11h, 11i, and 11v revealing enormous change in molecular structure, predominantly observed as a loss in aliphatic carbon (~ 10 to 90 ppm) and a relative gain in aromatic carbon at (~ 130 ppm). Right: ^{1}H solid state NMR spectra of Tagish Lake fragments 5b, 11h, 11i, and 11v revealing the systematic reduction in aliphatic H and the growth of aromatic H that correlates with the molecular changes observed in the ^{13}C solid state NMR spectra.

IOM: Transmission electron microscopy (TEM)

TEM characterization of samples 5b, 11b and a previous Tagish Lake sample (main text: Table 1 and Figure 1, (*8*)) was performed with a JEOL 2200FS field emission microscope operating at 200kV at the U.S. Naval Research Laboratory (NRL). Globules were easily distinguished from the non-globule IOM in STEM high-angle annular dark field (HAADF) images (Fig. S3). The observed abundance of globules was significantly greater in 5b than in 11v: 7.5% vs 0.9% area fraction, respectively. Globules for targeted STXM analysis (see next section) were located first by TEM, under conditions intended to minimize any electron-beam-induced alteration of the carbon chemistry, i.e., bright-field TEM imaging with minimal

beam exposure time, at low magnification with a deconverged beam and small condenser aperture. De Gregorio et al. (*48*) showed that this low-dose imaging protocol had a negligible effect on IOM from the Murchison chondrite meteorite.

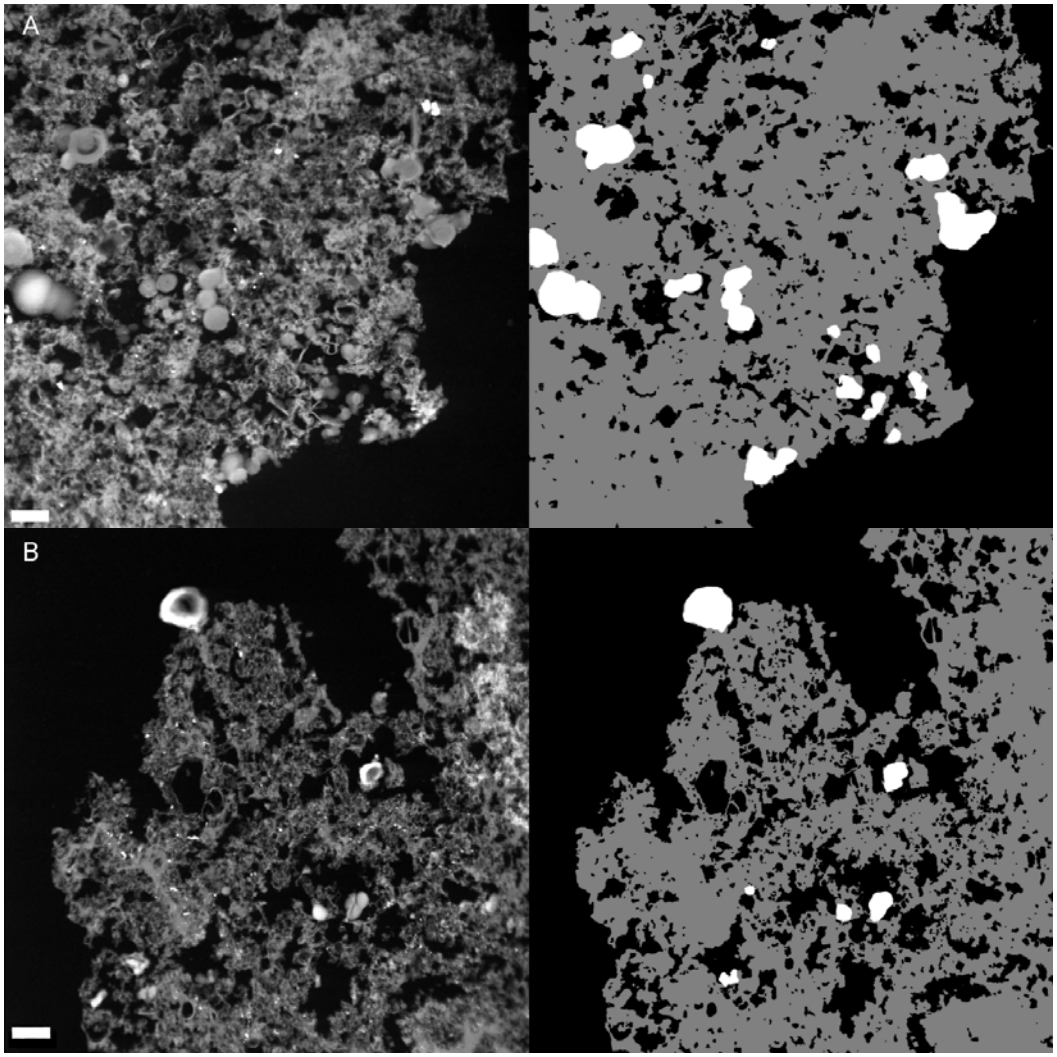

Figure S3. HAADF STEM images of samples 5b (A) and 11v (B), with corresponding image masks showing the location of globules (white). The scale bars are 0.5 μm.

IOM: C-, N-, and O-XANES analyses

Following TEM analysis, carbon, nitrogen, and oxygen X-ray absorption near edge structure (XANES) spectra were obtained on microtomed (to ~ 150 nm thick) samples of Tagish IOM that were transferred to SiO coated TEM grids. All XANES experiments were performed in transmission mode

using the scanning transmission X-ray microscope (STXM) located at beam line 5.3.2 at the Advanced Light Source, Lawrence Berkeley Laboratory (*24*). This microscope employs a bending magnet for soft X-ray generation providing a useful energy range of ~ 250 to 700 eV (spanning the C-, N-, and O-XANES regions). Submicron focusing is performed with a Fresnel Zone Plate objective and an order sorting aperture- providing spatial resolution down to 25 nm. Energy selection is obtained with a spherical grating monochromator with a resolution of 5000 eV/ΔeV. All analyses were performed using the multi-spectral imaging protocol, and XANES spectra are summed over 100's of voxels.

A total of 42 nanoglobules were analyzed from IOM from samples 5b (N = 15), 11v (N = 12) and a previous Tagish Lake sample (N = 15; main text: Table 1 and Figure 1, (*8*)), respectively. Most globules showed similar C-XANES spectra to that of normal (non-globule) IOM, but a fraction showed much more aromatic functionality, based on a dominant, broad absorption at ~285 eV (Figure S4). The fraction of such aromatic globules is slightly lower in sample 5b (3 out of 15 globules) than in the other, more altered, samples 11v (6 out of 12) and the previous one (5 out of 15), suggesting that either aromatic globules are generated or IOM-like globules are destroyed during alteration. However, since the globule sample size is small, the observed population variation between the Tagish Lake samples is negligible if Poisson statistical uncertainties are considered.

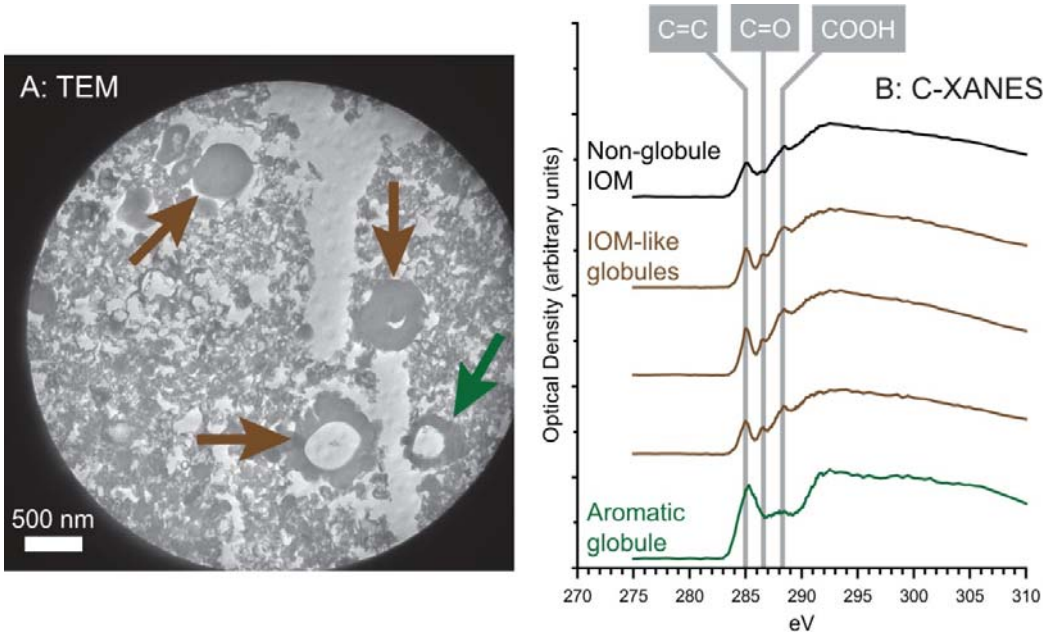

Figure S4. A) TEM bright-field image of IOM from Tagish Lake sample 5b with nanoglobules selected for STXM analysis indicated by arrows. B) C-XANES spectra of 5b IOM and nanoglobules.

IOM: Secondary ion mass spectrometry (SIMS)

SIMS measurements were made in imaging mode with a Cameca NanoSIMS 50L ion microprobe at the Carnegie Institution of Washington. In a first set of analyses, a 20 pA <300nm Cs+ primary ion beam was rastered over 25×25 μm^2 or 40×40 μm^2 areas of microtomed IOM slices and negative secondary ions of ^{1}H, ^{2}H and ^{13}C were simultaneously detected in multicollection. A total of 4000 μm^2 of 5b IOM and 1800 μm^2 of 11v IOM were analyzed. In a second analysis session, additional IOM regions were analyzed for H, C and N isotopes. For these measurements, a 1-2pA, ~200 nm diameter Cs^+ beam was used to generate images of ^{1}H, ^{2}H, ^{12}C, ^{13}C, $^{12}C^{14}N$, $^{12}C^{15}N$ and ^{28}Si negative secondary ions in multicollection. CN^- is commonly used for N-isotopic analysis in SIMS because of the high secondary ion yield for this molecule in the presence of both C and N. A mass-resolving power sufficient to resolve important isobaric interferences at mass 26 and 27 was used. A total of 6800 μm^2 of 5b IOM and 1500 μm^2 of 11v IOM were analyzed. Isotopic ratios for sub-regions of ion images were quantitatively determined and isotopic ratio images generated with the L'image software package (L. R. Nittler, Carnegie Institution). A terrestrial standard with composition $C_{30}H_{50}O$ and well-characterized IOM from the QUE 99177 carbonaceous chondrite (*8*) were used as isotopic standards. Unfortunately, count rates for H isotopes were too low under the conditions used for the second set of analyses so reliable H- and N-isotopic data are not available for the same IOM regions. The distribution of D/H ratios in sub-micron regions for 5b and 11v IOM is shown in Figure S5.

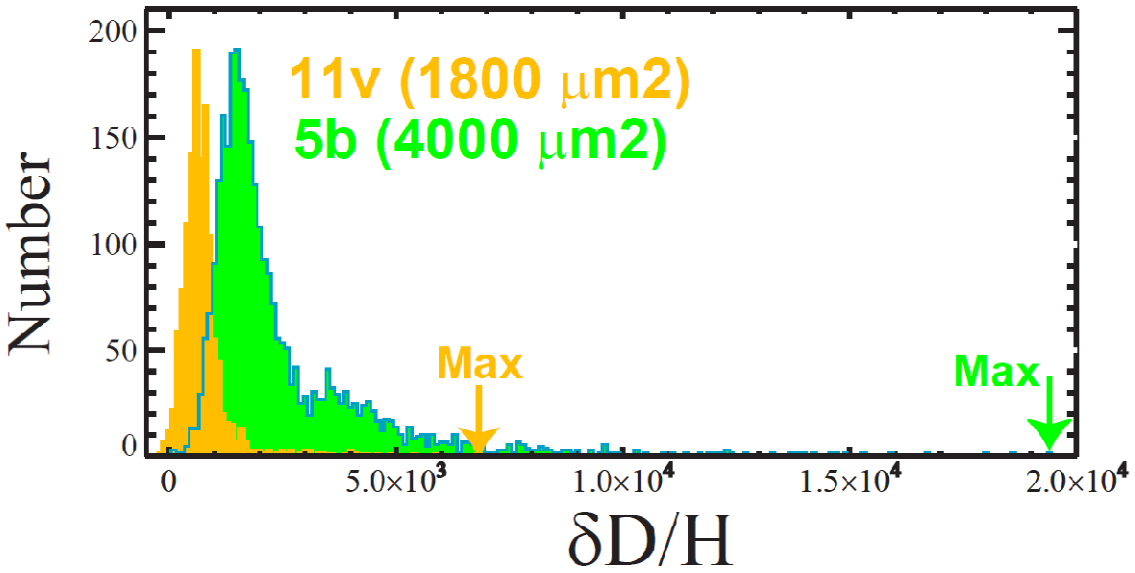

Figure S5. The distribution of D/H ratios in sub-micron regions of IOM separates from specimens 5b and 11v.

X-ray diffraction

A sample of each specimen was ground by hand under acetone in an agate mortar and pestle to produce a fine-grained powder. Powder XRD data were collected using a Rigaku Ultima IV Power Diffractometer housed in the Department of Earth and Atmospheric Sciences, University of Alberta. The instrument is equipped with a Co tube and a high-speed Si strip detector. We used Co *K*α radiation (λ = 1.7903 Å) , a step size of 0.02°2θ over the range 5-80°2θ, and 0.3 s count time per step. Samples were top loaded onto round Al holders (or glass where necessary) and spun at 0.5 Hertz. The detection limit for mineral phases is estimated at 1 wt%, and the absolute error is approximately 2 wt%. Phase identification and semi-quantitative phase abundances were determined by Rietveld refinement using the WPF module of JADE 9.0 software from MDI. Rietveld refinement uses nonlinear least-squares optimization to fit the data with a calculated model that is based on powder diffraction patterns taken from the International Centre for Diffraction Data Powder Diffraction File database (ICDD-PDF). Most of the samples were found to contain abundant clay minerals, for which no ideal structure model exists, and an amorphous phase not identifiable by the XRD.

EPMA analysis

Major and minor element concentrations in polished samples of each specimen were obtained by electron probe microanalysis (EPMA) using a JEOL 8900 Superprobe and Cameca SX100 housed in the Department of Earth and Atmospheric Sciences, University of Alberta. Both instruments were operated at 1-2 μm diameter focused electron beam with a current of 20 nA and an accelerating voltage of 20 kV. Natural minerals such as chromite, albite, diopside, etc. were used as external standards (*49*) for both instruments. Data reduction was performed using the Φ(rZ) correction (*50*). The instrument calibration was deemed successful when the composition of secondary standards was reproduced within the error margins defined by the counting statistics. Prior to the EPMA analyses chips of each specimen were prepared into 1 inch diameter mounts using Buehler EPOKWICK two part epoxy and then polished on a Logitech WG2 polishing unit with pellon polishing pads, diamond paste 6, 3, and 1 micron and Engis OS type 1V lubricant.

References and Notes

1. E. R. D. Scott, A. N. Krot, in *Treatise on Geochemistry,* H. D. Holland, K. K. Turekian, Eds. (Elsevier Pergamon, Oxford, 2007), vol. 1, pp. 1–72.

2. I. Gilmour, in *Treatise on Geochemistry,* H. D. Holland, K. K. Turekian, Eds. (Elsevier Pergamon, Oxford, 2003), vol. 1, pp. 269–290.

3. O. Botta, J. L. Bada, *Surv. Geophys.* **23**, 411 (2002).

4. J. R. Cronin, S. Pizzarello, D. P. Cruikshank, in *Meteorites and the Early Solar System,* J. F. Kerridge, M. S. Matthews, Eds. (Univ. of Arizona Press, Tucson, AZ, 1988), pp. 819–857.

5. H. Busemann *et al*., Interstellar chemistry recorded in organic matter from primitive meteorites. *Science* **312**, 727 (2006).

6. S. A. Sandford *et al*., Organics captured from comet 81P/Wild 2 by the Stardust spacecraft. *Science* **314**, 1720 (2006).

7. J. Duprat *et al*., Extreme deuterium excesses in ultracarbonaceous micrometeorites from central Antarctic snow. *Science* **328**, 742 (2010).

8. C. M. O. D. Alexander, M. Fogel, H. Yabuta, G. D. Cody, The origin and evolution of chondrites recorded in the elemental and isotopic compositions of their macromolecular organic matter. *Geochim. Cosmochim. Acta* **71**, 4380 (2007).

9. C. F. Chyba, P. J. Thomas, L. Brookshaw, C. Sagan, Cometary delivery of organic molecules to the early Earth. *Science* **249**, 366 (1990).

10. Y. Huang, M. R. Alexandre, Y. Wang, Structure and isotopic ratios of aliphatic side chains in the insoluble organic matter of the Murchison carbonaceous chondrite. *Earth Planet. Sci. Lett.* **259**, 517 (2007).

11. Y. Oba, H. Naraoka, Carbon isotopic composition of acetic acid generated by hydrous pyrolysis of macromolecular organic matter from the Murchison meteorite. *Meteorit. Planet. Sci.* **41**, 1175 (2006).

12. L. Remusat, S. Derenne, F. Robert, H. Knicker, New pyrolytic and spectroscopic data on Orgueil and Murchison insoluble organic matter: A different origin than soluble? *Geochim. Cosmochim. Acta* **69**, 3919 (2005).

13. Information on materials and methods is available as supporting material on *Science* Online.

14. Hydrothermal alteration occurred early in the history of the carbonaceous chondrite parent bodies owing to accumulation of the heat of radioactive decay, so that liquid water was transiently present and percolated through the mineral matrix. The evidence for this process is preserved in mineral alterations. Furthermore, in the interior of the parent body, the temperature and pressure can rise high enough to produce hydropyrolysis of organic material.

15. M. E. Zolensky *et al*., Mineralogy of Tagish Lake: An ungrouped type 2 carbonaceous chondrite. *Meteorit. Planet. Sci.* **37**, 737 (2002).

16. T. Hiroi, M. E. Zolensky, C. M. Pieters, The Tagish Lake meteorite: A possible sample from a D-type asteroid. *Science* **293**, 2234 (2001).

17. M. M. Grady, A. B. Verchovsky, I. A. Franchi, I. P. Wright, C. T. Pillinger, Light dement geochemistry of the Tagish Lake CI2 chondrite: Comparison with CI1 and CM2 meteorites. *Meteorit. Planet. Sci.* **37**, 713 (2002).

18. S. Pizzarello *et al*., The organic content of the Tagish Lake meteorite. *Science* **293**, 2236 (2001).

19. G. Kminek, O. Botta, D. P. Glavin, J. L. Bada, Amino acids in the Tagish Lake meteorite. *Meteorit. Planet. Sci.* **37**, 697 (2002).

20. K. Nakamura-Messenger, S. Messenger, L. P. Keller, S. J. Clemett, M. E. Zolensky, Organic globules in the Tagish Lake meteorite: Remnants of the protosolar disk. *Science* **314**, 1439 (2006).

21. R. K. Herd, C. D. K. Herd, *Lunar Planet. Sci.* **XXXVIII**, abs. 2347 (2007).

22. P. G. Brown *et al*., The fall, recovery, orbit, and composition of the Tagish Lake meteorite: A new type of carbonaceous chondrite. *Science* **290**, 320 (2000).

23. A. J. Brearley, in *Treatise on Geochemistry,* H. D. Holland, K. K. Turekian, Eds. (Elsevier Pergamon, Oxford, 2003), vol. 1, pp. 247–268.

24. A. L. D. Kilcoyne *et al*., Interferometer-controlled scanning transmission X-ray microscopes at the Advanced Light Source. *J. Synchrotron Radiat.* **10**, 125 (2003).

25. H. Yabuta, L. B. Williams, G. D. Cody, C. M. O. Alexander, S. Pizzarello, The insoluble carbonaceous material of CM chondrites: A possible source of discrete organic compounds under hydrothermal conditions. *Meteorit. Planet. Sci.* **42**, 37 (2007).

26. G. D. Cody, C. M. O. D. Alexander, NMR studies of chemical structural variation of insoluble organic matter from different carbonaceous chondrite groups. *Geochim. Cosmochim. Acta* **69**, 1085 (2005).

27. M. C. Anguera *et al*., Regulation of folate-mediated one-carbon metabolism by 10-formyltetrahydrofolate dehydrogenase. *J. Biol. Chem.* **281**, 18335 (2006).

28. G. K. Smith, W. T. Mueller, L. J. Slieker, C. W. DeBrosse, S. J. Benkovic, Direct transfer of one-carbon units in the transformylations of de novo purine biosynthesis. *Biochemistry* **21**, 2870 (1982).

29. D. Deamer, J. P. Dworkin, S. A. Sandford, M. P. Bernstein, L. J. Allamandola, The first cell membranes. *Astrobiology* **2**, 371 (2002).

30. Y. S. Huang *et al*., Molecular and compound-specific isotopic characterization of monocarboxylic acids in carbonaceous meteorites. *Geochim. Cosmochim. Acta* **69**, 1073 (2005).

31. G. Yuen, N. Blair, D. J. Des Marais, S. Chang, Carbon isotope composition of low molecular weight hydrocarbons and monocarboxylic acids from Murchison meteorite. *Nature* **307**, 252 (1984).

32. R. F. Dias, K. H. Freeman, M. D. Lewan, S. G. Franks, $\delta^{13}C$ of low-molecular-weight organic acids generated by the hydrous pyrolysis of oil-prone source rocks. *Geochim. Cosmochim. Acta* **66**, 2755 (2002).

33. D. P. Glavin, J. P. Dworkin, Enrichment of the amino acid L-isovaline by aqueous alteration on CI and CM meteorite parent bodies. *Proc. Natl. Acad. Sci. U.S.A.* **106**, 5487 (2009).

34. R. Bowen, in *Isotopes in the Earth Sciences*, R. Bowen, Ed. (Kluwer, New York, 1988), pp. 452–469.

35. D. P. Glavin, M. P. Callahan, J. P. Dworkin, J. E. Elsila, The effects of parent body processes on amino acids in carbonaceous chondrites. *Meteorit. Planet. Sci.* **45**, 1948 (2010).

36. J. R. Cronin, S. Pizzarello, S. Epstein, R. V. Krishnamurthy, Molecular and isotopic analyses of the hydroxy acids, dicarboxylic acids, and hydroxicarboxylic acids of the Murchison meteorite. *Geochim. Cosmochim. Acta* **57**, 4745 (1993).

37. E. T. Peltzer, J. L. Bada, G. Schlesinger, S. L. Miller, The chemical conditions on the parent body of the murchison meteorite: Some conclusions based on amino, hydroxy and dicarboxylic acids. *Adv. Space Sci.* **4**, 69 (1984).

38. S. Pizzarello, M. Zolensky, K. A. Turk, Nonracemic isovaline in the Murchison meteorite: Chiral distribution and mineral association. *Geochim. Cosmochim. Acta* **67**, 1589 (2003).

39. E. T. Peltzer, J. L. Bada, α-Hydroxycarboxylic acids in the Murchison meteorite. *Nature* **272**, 443 (1978).

40. J. E. Elsila, J. P. Dworkin, M. P. Bernstein, M. P. Martin, S. A. Sandford, Mechanisms of amino acid formation in interstellar ice analogs. *Astrophys. J.* **660**, 911 (2007).

41. Where given, the errors are half the difference (standard error of the mean) between the compositions of two residues prepared from two separate aliquots of each specimen. Typically, the differences in elemental ratios and isotopic compositions are larger than the intrinsic measurement precisions. Where only one measurement was made, the uncertainties of the other samples are a guide to the likely uncertainties.

42. D. P. Glavin *et al*., Amino acid analyses of Antarctic CM2 meteorites using liquid chromatography-time of flight-mass spectrometry. *Meteorit. Planet. Sci.* **41**, 889 (2006).

43. J. E. Elsila, D. P. Glavin, J. P. Dworkin, Cometary glycine detected in samples returned by Stardust. *Meteorit. Planet. Sci.* **44**, 1323 (2009).

44. G. Docherty, V. Jones, R. P. Evershed, Practical and theoretical considerations in the gas chromatography/combustion/isotope ratio mass spectrometry $\delta^{13}C$ analysis of small polyfunctional compounds. *Rapid Commun. Mass Spectrom.* **15**, 730 (2001).

45. J. P. Bradley, L. P. Keller, K. L. Thomas, T. B. Vander Wood, D. E. Brownlee, *Lunar Planet. Sci.* **XXIV**, abs. 1087 (1993).

46. Y. Wang, Y. Huang, C. M. O. D. Alexander, M. Fogel, G. Cody, Molecular and compound-specific hydrogen isotope analyses of insoluble organic matter from different carbonaceous chondrite groups. *Geochim. Cosmochim. Acta* **69**, 3711 (2005).

47. M. J. Wooller *et al*., Quantitative paleotemperature estimates from $\delta^{18}O$ of chironomid head capsules preserved in arctic lake sediments. *J. Paleolimnol.* **31**, 267 (2004).

48. B. T. De Gregorio *et al*., Isotopic anomalies in organic nanoglobules from Comet 81P/Wild 2: Comparison to Murchison nanoglobules and isotopic anomalies induced in terrestrial organics by electron irradiation. *Geochim. Cosmochim. Acta* **74**, 4454 (2010).

49. E. Jarosewich, *J. Res. Natl. Inst. Stand. Technol.* **107**, 681 (2002).

50. J. T. Armstrong, *Microbeam Anal.* **4**, 177 (1995).